International Journal of *Molecular Sciences*

MDPI

Supplementary Material

Investigations of the Kinetics and Mechanism of Reduction of a Carboplatin Pt(IV) Prodrug by the Major Small-Molecule Reductants in Human Plasma

One supporting table (Table S1) and six supporting figures (Figures S1-S6) are included in the Supplementary Material.

Table S1. Observed second-order rate constants k' for the reduction of *cis,trans*-$[Pt(cbdca)(NH_3)_2Cl_2]$ by Cys and GSH as a function of pH at 25.0 °C and μ = 1.0 M.

Thiol	pH	$k'/M^{-1}s^{-1}$
Cys	2.47	0.79 ± 0.02
	2.67	1.15 ± 0.03
	2.93	1.62 ± 0.04
	3.23	2.50 ± 0.06
	3.57	5.16 ± 0.15
	4.01	11.9 ± 0.2
	4.47	32.9 ± 0.7
	5.07	127 ± 3
	5.72	549 ± 9
	6.29	(1.96 ± 0.06) x 10^3
	6.94	(8.2 ± 0.2) x 10^3
	7.40	(1.93 ± 0.06) x 10^4
	7.90	(3.70 ± 0.09) x 10^4
	8.43	(6.2 ± 0.1) x 10^4
	8.60	(8.0 ± 0.2) x 10^4
	9.09	(1.22 ± 0.03) x 10^5
	9.48	(1.66 ± 0.04) x 10^5
	9.96	(2.37 ± 0.08) x 10^5
	10.83	(3.22 ± 0.15) x 10^5
	11.24	(3.86± 0.16) x 10^5
GSH	2.47	0.54 ± 0.02
	2.67	0.82 ± 0.02
	2.93	1.19 ± 0.03
	3.23	1.96 ± 0.04
	3.57	2.99 ± 0.06
	4.01	5.36 ± 0.15

4.47	14.4 ± 0.3
5.07	59.0 ± 1.5
5.72	272 ± 8
6.29	(1.02 ± 0.03) x 10^3
6.94	(4.34 ± 0.09) x 10^3
7.40	(1.01 ± 0.03) x 10^4
7.90	(2.38 ± 0.06) x 10^4
8.43	(8.15 ± 0.19) x 10^4
8.60	(1.00 ± 0.03) x 10^5
9.09	(1.74 ± 0.04) x 10^5
9.48	(2.41 ± 0.06) x 10^5
9.96	(2.59 ± 0.08) x 10^5
10.34	(2.74 ± 0.08) x 10^5
10.83	(3.30 ± 0.08) x 10^5
11.24	(2.83 ± 0.08) x 10^5

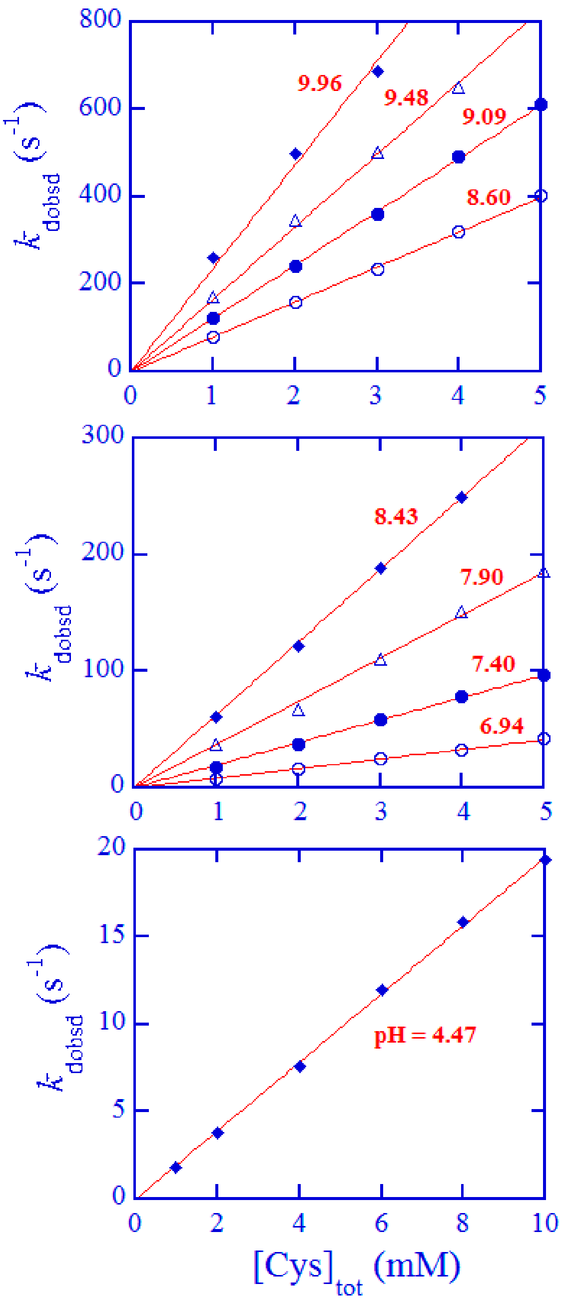

Figure S1. Plots of k_{obsd} versus $[\mathrm{Cys}]_{\mathrm{tot}}$ for the reduction of *cis,trans*-$[\mathrm{Pt(cbdca)(NH_3)_2Cl_2}]$ by Cys at 25.0 °C, μ = 1.0 M in buffer solutions at pH between 4.47 and 9.96 as denoted by the red numbers above each line.

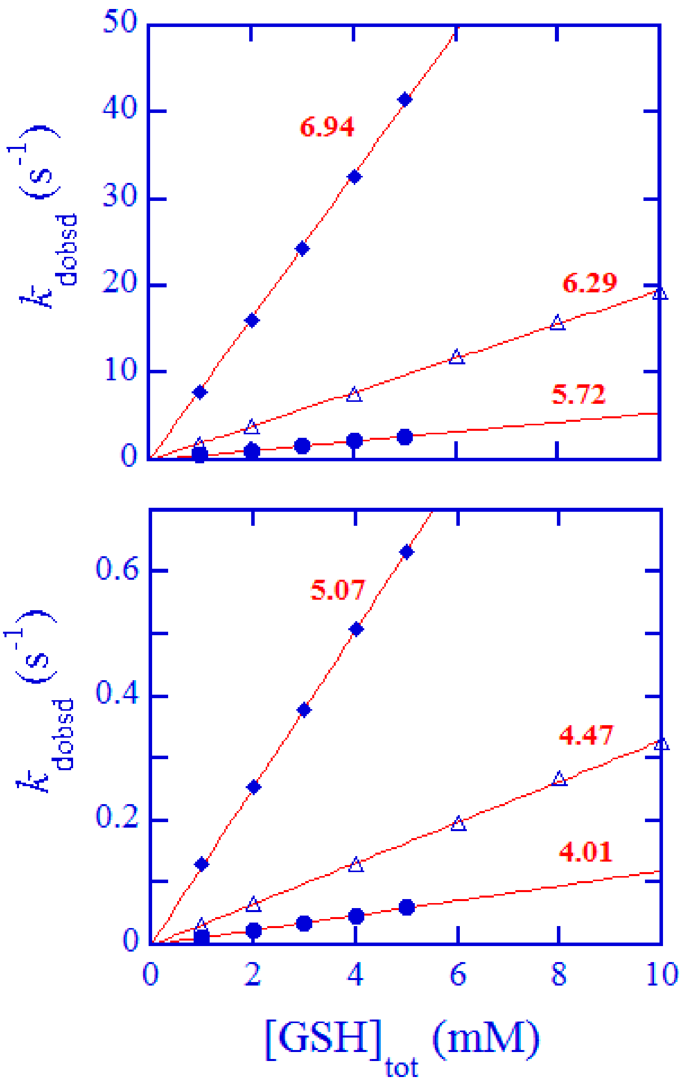

Figure S2. Plots of k_{obsd} versus $[GSH]_{tot}$ for the reduction of *cis,trans*-[Pt(cbdca)$(NH_3)_2Cl_2$] by GSH at 25.0 °C, μ = 1.0 M in buffer solutions at pH between 4.01 and 6.94 as denoted by the red numbers above each line.

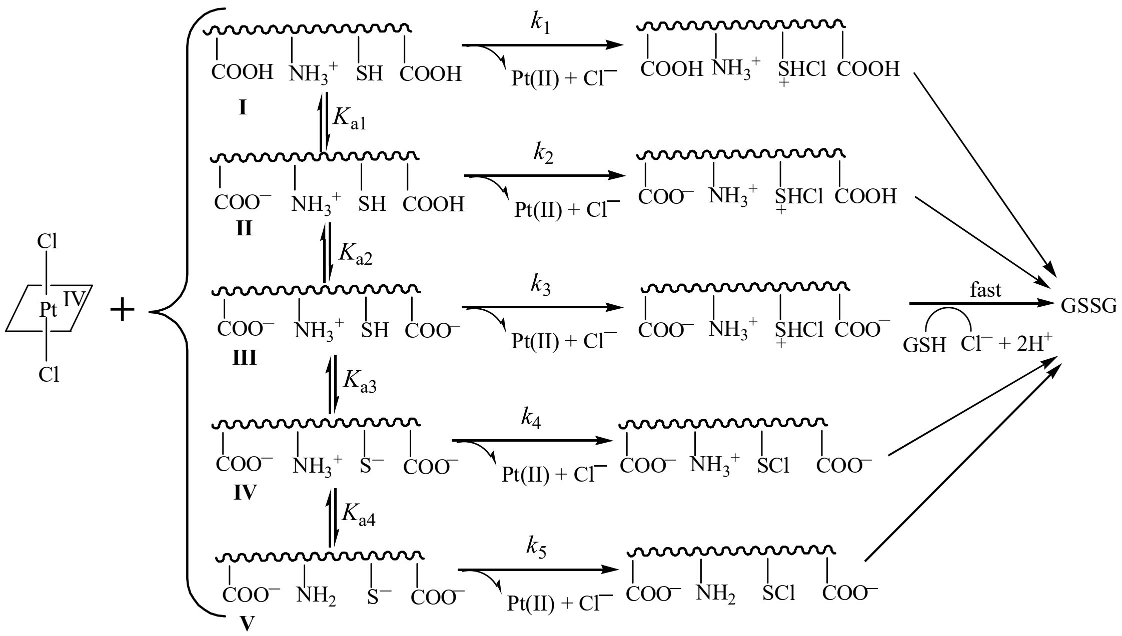

Pt(IV) = *cis,trans*-[Pt(cbdca)$(NH_3)_2Cl_2$]; Pt(II) = *cis*-[Pt(cbdca)$(NH_3)_2$]

Figure S3. Reaction mechanism proposed for the reduction of *cis,trans*-[Pt(cbdca)$(NH_3)_2Cl_2$] by GSH.

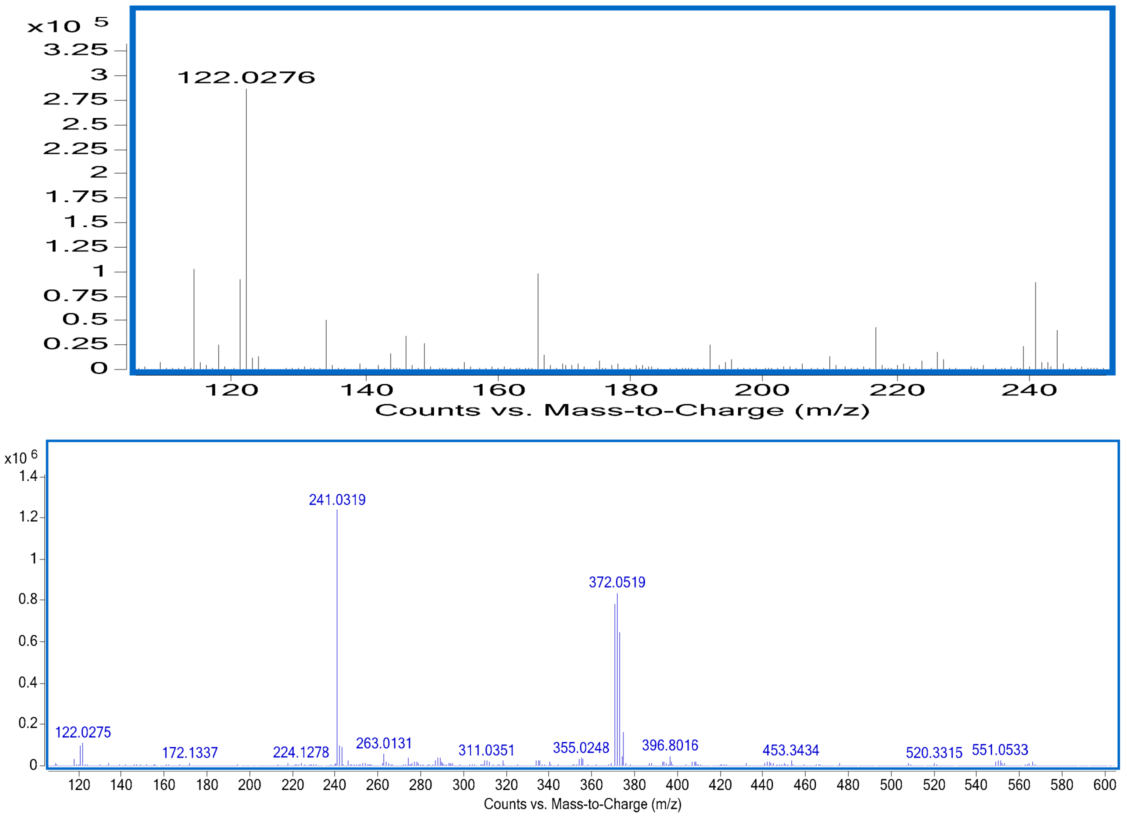

Figure S4. High-resolution mass spectra. (Top): 10 mM L-Cys in 10 mM HAc. (Bottom): A reaction mixture of 10 mM L-Cys with 1 mM *cis,trans*-[Pt(cbdca)$(NH_3)_2Cl_2$] in 10 mM HAc after a reaction time of 5 min.

Peak assignments: *m*/*z* = 122.027 for Cys·H$^+$; *m*/*z* = 241.03 for CysS-SCys·H$^+$; *m*/*z* = 372.05 for carboplatin·H$^+$ (or *cis*-[Pt(cbdca)$(NH_3)_2$]·H$^+$).

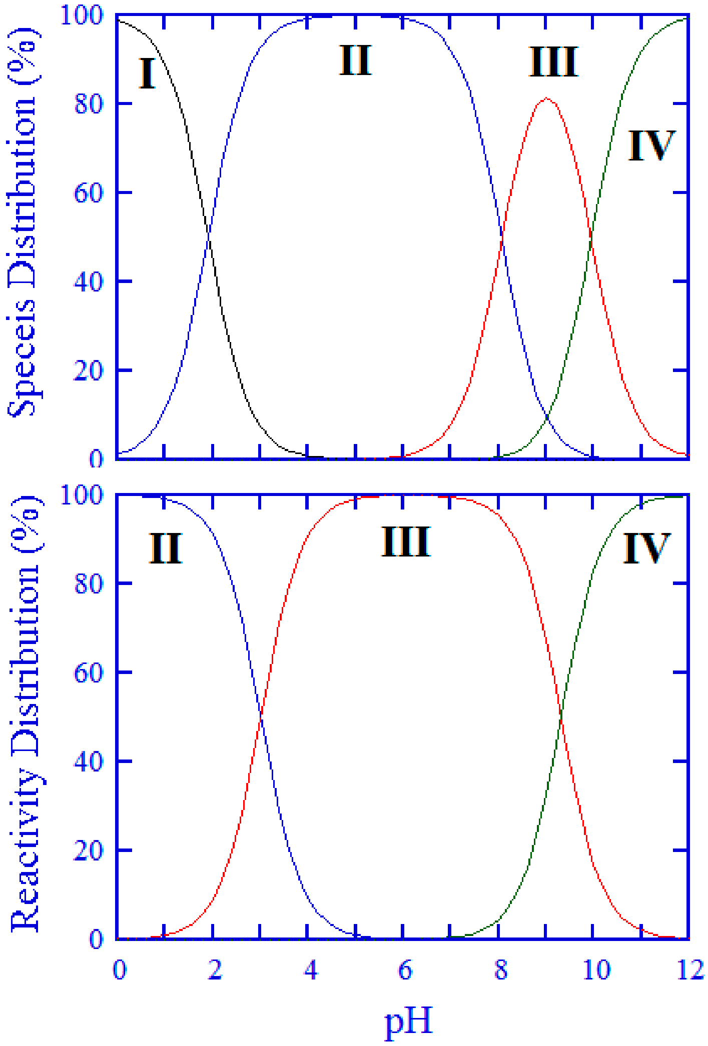

Figure S5. (Top): Distribution diagram for the various Cys protolytic species versus pH calculated from pK_{a1} = 1.9, pK_{a2} = 8.07, and pK_{a3} = 9.95. (Bottom): Reactivity fraction of the Cys species in the reduction of *cis,trans*-[Pt(cbdca)(NH_3)$_2$$Cl_2$] versus pH. The p$K_a$ values and the rate constants in Table 2 were utilized to generate this diagram. Structures of the Cys species **I – IV** are given in Figure 7 in the main text.

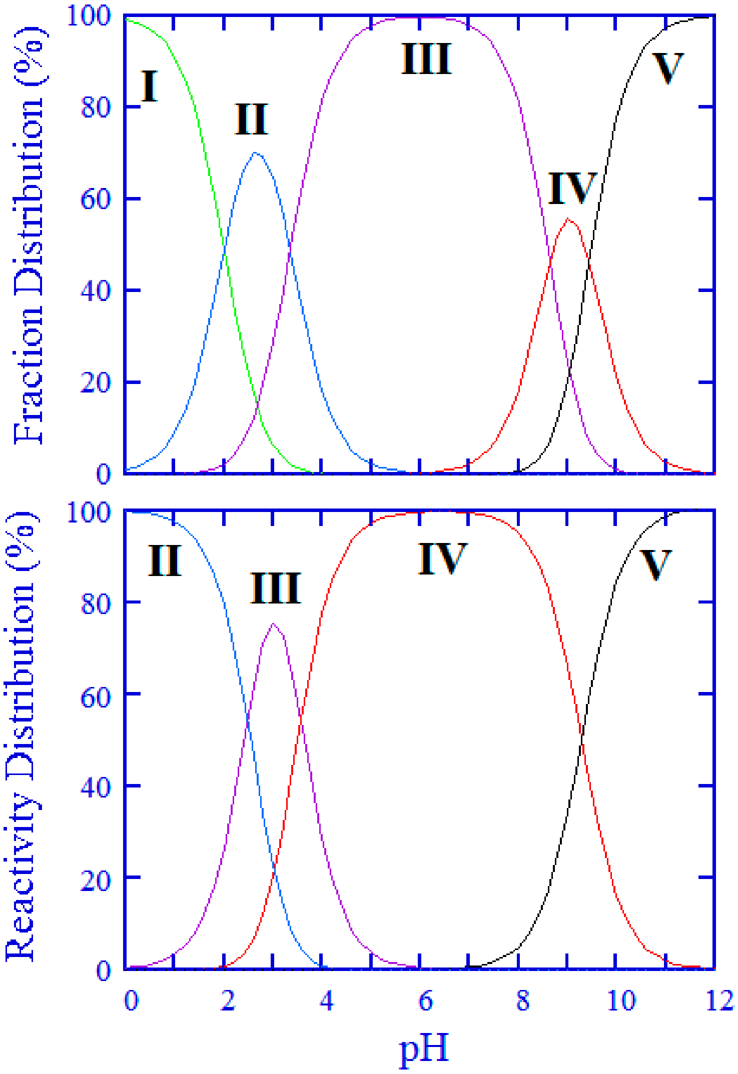

Figure S6. (Top): Distribution diagram for the various GSH protolytic species versus pH calculated from pK_{a1} = 2, pK_{a2} = 3.35, pK_{a3} = 8.64 and pK_{a4} = 9.44. (Bottom): Reactivity fraction of the GSH species in the reduction of *cis,trans*-[Pt(cbdca)(NH_3)$_2$$Cl_2$] versus pH. The p$K_a$ values and the rate constants in Table 2 were utilized to generate this diagram. Structures of the GSH species **I** – **V** are given in Figure S3.